Comparison of control methods for 2D industrial cranes

Mohammad Rasool Mojallizadeh, Bernard Brogliato, Christophe Prieur

Comparison of control methods for 2D industrial cranes*

Mohammad Rasool Mojallizadeh[1], Bernard Brogliato[1] and Christophe Prieur[2]

***Abstract*— This paper aims to review and compare some methods used to control 2D overhead cranes. The properties of the controllers are categorized based on their structure, feedback type (open-loop, collocated, and noncollocated), and their stability (local, global, regulation and tracking). Subsequently, a new model is used to describe the system's behavior more accurately. The model consists of a pendulum with a large number of links attached to a cart, allowing to study global nonlinearities as well as cables' flexibility and vibration, simultaneously. The controllers are then studied by extensive numerical simulations under the regulation and tracking scenarios.**

I. INTRODUCTION

Overhead cranes (OC) are widely employed in construction sites and warehouses to manipulate heavy loads. These machines are mainly composed of a moving cart with a hook or tool attached to the cart via some cables. For a satisfactory operation, an appropriate control method should be implemented on cranes to ensure fast and accurate positioning with as small as possible payload sway. Satisfying these objectives may not be straightforward since OCs are known as underactuated systems with complex nonlinear dynamics. Moreover, there is always a trade-off between operation time and payload sway [1]. Several types of control methods have been proposed in the literature to address the mentioned control objectives. The first and the simplest category belongs to the open-loop (OL) schemes where no feedback or sensor is required by the control algorithm. While OL approaches can provide simplicity and economic solutions, they suffer from severe sensitivity to the uncertainties. Zero-vibration (ZV) and zero-vibration-derivative (ZVD) are two known examples of such open-loop paradigms [2]. To solve the drawbacks of the OL schemes, closed-loop (CL) controllers have been introduced. The first group of the CL controllers only requires the collocated feedback, i.e., cart coordinates. Other CL controllers need underactuated feedback information, including the sway angles or payload coordinates [3]. OCs are mostly designed and analyzed based on simplified models such as single- [4] or double-pendulum [5] systems. These models can describe the global nonlinearities corresponding to the sway angles. However, high-frequency vibrations caused by the hoisting cables cannot be modeled with such models. Hence, infinite-dimensional models leading to partial differential equations are proposed which are in turn difficult to be used when dealing with global nonlinearities [6], [7], [8].

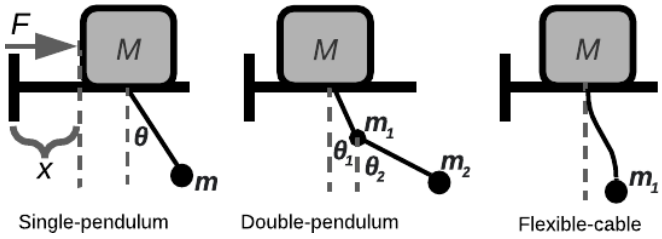

Fig. 1. Different approaches in modeling an overhead crane

The main contribution of this paper is to take into account a large number of links with damping and flexibility on the joints to form a new model for capturing both global nonlinearities and cables' dynamics, simultaneously. Since several sway angles can be considered for such a model, the appropriate sway angle measurement has also been addressed in this study to implement the controllers designed for the single- and double-pendulum systems. Furthermore, a unified gain tuning approach has been developed to tune the parameters of the controllers in a unified manner leading to fair comparisons. Subsequently, a complete analysis of the control methods has been provided and their responses are compared on the considered model using numerical simulations. In the leftover of this paper, a review of the controllers are presented in Section II, the numerical simulations are provided in Section IV, and, finally, Section V concludes the paper.

II. CASE STUDY: AN OVERHEAD CRANE IN 2D SPACE

The principal operation of an OC is usually described by a pendulum attached to a cart that moves on a line or surface. Depending on the number/type of the links, three modeling schemes can be found in the literature as shown in Fig. 1. The simplest one is the single-pendulum approach with a rigid link. However, in the presence of heavy hooks, the double-pendulum model provides better accuracy. Another approach is to take into account the flexibility of the cable to model the vibrations corresponding to the cables' flexibility.

Single- and double-pendulum models provide straightforward solutions to model the global nonlinearities corresponding to the primary and secondary sway angles. However, it is not possible to study the oscillations of the cable using these models. On the other hand, the infinite-dimensional models developed for the cables' flexibility are inherently local and linear (*e.g.*, string or wave equations) and hard to use to control the global nonlinearities [7], [8]. In this paper

*This work was supported by IRT-NanoElec project Levage, Grenoble.

[1]Univ. Grenoble Alpes, INRIA, CNRS, Grenoble INP, LJK, 38000 Grenoble, France mohammad-rasool.mojallizadeh@inria.fr, bernard.brogliato@inria.fr

[2]Université Grenoble Alpes, CNRS, Grenoble-INP, GIPSA-lab, F-38000, Grenoble, France Christophe.Prieur @gipsa-lab.fr

a model is built which tentatively combines some features of both methods. We use it to compare several types of controllers. This model consists of a pendulum/cable system with several links (20 in our case). Both global nonlinear dynamics, as well as some vibrations corresponding to the cable's flexibility, can be taken into account. The mentioned model has been implemented based on the following assumptions:

- The model is composed of a 20-link pendulum such that 19 links model the flexibility of the cable, and the last one represents the secondary sway corresponding to the hook. While more links may improve the accuracy of the model, it makes the simulations too slow to be used.
- The masses connected to the last and next to the last link are equal to the masses of the payload and the hook, respectively. The weight of the cable is distributed on other links uniformly.
- The model is developed for 2D operational space.

III. Summary of the studied controllers

According to the literature, the controllers used to control OCs follow the following structure:

$$F = \{FF\} + \{P\} + \{D\} + \{I\} \tag{1}$$

where F is the force applied to the cart, $\{FF\}$, $\{P\}$, $\{D\}$, and $\{I\}$ denote the feedforward, proportional, derivative and integrative terms. These terms are summarized in Table I. In this table, m_t is total mass of the crane, a_d is the payload reference trajectory. $\mathrm{conv}(A, B)$ is the convolution of the vectors A and B, P_1 and P_2 are two vectors containing two and three impulses, respectively. Moreover, $e_x = x - x_d$, $e_v = v - v_d$, $\chi = e_x + \lambda \sin(\theta)$, $x(t)$ and $v(t)$ are cart position and velocity, respectively, x_d and v_d are the references for the payload position and velocity, respectively. Note that the controllers have some parameters $k_p, k_d, k_i \xi, \phi, k_a, k_q, k_{\phi 1}, k_{\phi 2}, \alpha_1, \alpha_2, \alpha_3, \lambda, \zeta \in \mathbb{R}^+$ that need to be tuned, also one has $\alpha_1 \alpha_4 = \alpha_2 \alpha_3 - \alpha_3 \left(\frac{\alpha_2}{2} + \frac{\sqrt{\alpha_2^2 + 4\alpha_1}}{2} \right)$. The controllers in this topic are designed for one of the systems shown in Fig. 1, and depending on the model, the sway angles θ, θ_1, and θ_2 can be measured as shown according to this figure. It should be noted that among the controllers, the sliding-mode controllers (SMC) do not follow the structure shown in (1) and are composed of nonlinear combinations of several terms. One may refer to the references cited in Table I for more details. The SMC designed for the single-pendulum system has six parameters $c_1, c_2, c_3, c_4, k, \eta \in \mathbb{R}^+$ while the one designed for the double-pendulum one has five parameters $\lambda, \alpha, \beta, K, c \in \mathbb{R}^+$. The SMC designed for the double-pendulum system uses a linear filter with the parameter c to calculate the angular accelerations [9].

A. Comparison of the controllers

From Table I one can see that among the closed-loop methods, the tracking controllers use the feed-forward terms which is not the case for the regulation ones. Moreover, the type of stability proof for each method is listed in the last column. It can be seen that each stability proof is provided for a specific model. Hence, implementing controllers on different models (like the 20-link pendulum model used in the simulations) may not necessarily lead to a stable implementation. Also, note that the global stability of the PD-PD method has not been guaranteed since it is designed based on the assumption that transversal and angular displacements are small. Note that the robust stability of the SMCs has been ensured in the presence of matched disturbances which is not the case for other controllers.

General specifications of the controllers are given in Table II. The controllers can be divided into three classes based on the type of feedback. The first category belongs to the open-loop schemes. The other one is the collocated control methods where the position of the cart and its time derivative are the only feedback information. Finally, the noncollocated strategies where the sway angles are also required to synthesize the control law. The number of required sensors and tuning parameters corresponding to each method has also been listed in this table.

Note that the noncollocated controllers are designed either for the single- or double-pendulum models. However, in this study, a 20-link pendulum is used as the case study which raises the question that which angles should be measured for θ_1 and θ_2, corresponding to the double-pendulum system's angles shown in Fig. 1. To the best of the authors' knowledge, this problem has not been studied elsewhere. In this work, it is assumed that the first and the last angles (if the coordinates are considered as Fig. 1) correspond to θ_1 and θ_2, respectively. For the noncollocated methods where only a single angle feeds the controller, two different implementations have been considered with the first and the last angles as feedback. This issue can also be observed in real practical applications since several angles can be measured in a crane because of the cable's flexibility and the sensor position.

IV. Numerical simulations

Numerical simulations have been conducted to investigate the general behavior of the controllers on an OC with the parameters shown in Table III[1]. It is assumed that the 8 parallel cables can be modeled as a single cable with the modified parameters multiplied by 8 as shown in Table III. Some objective functions are defined for the ease of comparison as shown in Table IV. Note that, in this table, x_p is the payload position and n is the number of links. Since variable step size numerical solvers are used for the simulations, $\bar{L}_2$ and $\tilde{L}_2$ are scaled.

A. Optimization algorithms

As can be seen from Table II, the controllers' gains have to be tuned to ensure a fair comparison. This problem has not been addressed in the literature, and it is not clear how to formulate and solve that analytically because of its complexity.

[1]A toolbox is available upon the request of the first author (mohammadrasool.mojallizadeh@inria.fr) to reproduce all results.

TABLE I

STRUCTURE OF THE CONTROLLERS

Controller	feed-forward terms	proportional terms	derivative terms	integration terms	stability
Unshaped input [2]	$+m_t a_d$	—	—	—	no proof
ZV [2]	$+\text{conv}(m_t a_d, \bar{P}_1)$	—	—	—	no proof
ZVD [2]	$+\text{conv}(m_t a_d, \bar{P}_2)$	—	—	—	no proof
Collocated PD [10], [4]	—	$+k_p e_x(t)$	$+k_d e_v(t)$	—	GA1 & GA2
Noncollocated Quasi-PID [5]	—	$-k_p \tanh(e_x)$	$-k_d \tanh(e_v)$ $-k_{\phi 1} \tanh^2(\dot{\theta}_1) \tanh(e_v)$ $-k_{\phi 2} \tanh^2(\dot{\theta}_2) \tanh(e_v)$	$-k_i \tanh\left(\lambda^2 e_x + \lambda \int_0^t \tanh(e_x) dt\right)$	GA2
Noncollocated PD regulation [10]	—	$-k_p\big(e_x(t) - k_a \sin(\theta(t))\big)$	$-k_d\big(e_v(t) - k_a \dot{\theta}(t) \cos(\theta)\big)$	—	GA1
Collocated PD tracking [11]	$+m_t a_d$	$-k_p e_x(t)$ $-\dfrac{2\lambda\xi^2}{\xi^2 - e_x^2(t)} e_x(t)$	$-k_d e_v(t)$ $-\phi\,\text{sgn}(e_v(t))$	—	GA1
PD-PD [12]	—	$-\alpha_1 e_x(t)$ $-\alpha_3 \theta(t)$	$-\alpha_2 e_v(t)$ $-\alpha_4 \dot{\theta}(t)$	—	LI
SMC (see [13]) single-pendulum	—	discontinuous combination of proportional and derivative terms			GA1 & RM
SMC (see [14]) double-pendulum	—				GA2 & RM
PD energy [15]	—	$-k_p \tanh(\chi) - k_q \chi \times \dfrac{(x_d+\zeta)^2 - \varepsilon^2 + \chi\varepsilon}{((x_d+\zeta)^2 - \varepsilon^2)^2}$	$-k_d \dot{\chi}$	—	GA1
Coupling tracking [16]	$+m_t a_d$	$-k_p \int_0^t \zeta dt$	$-k_d \zeta + \lambda m_t \cos(\theta)\dot{\theta}$	—	GA1

GA1 and GA2 denote global asymptotic stability for the single- and double-pendulum systems, respectively.
LI indicates local stability based on the infinite dimensional model, and RM denotes robustness to matched uncertainties.

TABLE II

OVERVIEW OF THE CONTROLLERS.

Controller	Feedback	NoP	Case	Sensor
Unshaped input	open-loop	-	-	-
ZV	open-loop	-	-	-
ZVD	open-loop	-	-	-
Collocated PD	collocated	2	R	2
Noncollocated Quasi-PID	noncollocated	4	R	4
noncollocated PD	noncollocated	3	R	4
Collocated PD Tracking	collocated	5	T	2
PD-PD	noncollocated	3	R	4
SMC single-pendulum	noncollocated	6	R	4
SMC double-pendulum	noncollocated	5	R	6
PD energy	noncollocated	6	R	5
Coupling tracking	noncollocated	3	T	3

R: regulation, T: tracking, NoP: number of parameters

TABLE III

PARAMETERS OF THE CRANE USED IN THE SIMULATIONS

number of cables	8
cart mass	10tons
hook mass	13.6tons
payload mass	40tons
hook to load distance	1m
damping coefficient for the joints	0.2 × 8 (NM/(deg/s))
joint flexibility coefficient	0.1 × 8 NM/deg
cart to payload distance	10m
controller sampling time	50ms
simulation time	100s
delay in the feedback's path	100ms
force saturation bound	$\pm 10^5$N

TABLE IV

OBJECTIVE FUNCTIONS

variables	definition
$e_p = x_p - x_d$	Payload position error
$e_c = x_c - x_d$	Cart position error
$\tilde{L}_2(X) = 10^3 L_2(X)/\text{length}(X)$	$\tilde{L}_2$ norm
$\bar{L}_2(X) = 10^5 L_2(X)/\text{length}(X)$	$\bar{L}_2$ norm
$e_a(t) = \sum_{i=1}^{n} \lvert\theta_i(t)\rvert$	Total sway

In this study, some classical algorithms are used in a unified manner for all controllers to tune their parameters. The parameters are optimized for a double-pendulum system[2] in the presence of an initial sway $\theta_1(0) = -\theta_2(0) = 15$, a cart disturbance (a pulse force with period 20s and amplitude $\pm$19600N), damping on the cart ($1000v(t)$N to simulate a kind of friction between the cart and the surface), and the measurement noise (all measurements are affected by white noise with SNR=90dB) with the reference trajectory defined in Section IV-B. Three optimization algorithms, i.e., `PSO`, `fminunc` and `patternsearch` have been employed from MATLAB R2021b software package to minimize the following objective function:

$$\begin{aligned} J = &||e_p(t)||_{t\in[0,100]s} + 60||e_p(t)||_{t\in[16,100]s} \\ &+300||e_p(t)||_{t\in[33,100]s} \\ &+600||e_p(t)||_\infty + 0.05\sum_0^{10} |F(k) - F(k-1)| \end{aligned} \tag{2}$$

[2]The 20-link pendulum system cannot be directly used by the optimization algorithms to tune the parameter since it requires too much calculation time. The double-pendulum system has been used, instead, since it can model the double-pendulum effect corresponding to the presence of hook, and at the same time, it does not require too much calculation resources. The optimization on the double-pendulum model takes around 12 hours for all methods when using a computer whith `Intel Core i7-1080H` CPU and 32 GB RAM. This may take around a year when using the 20-link pendulum on the same PC.

where $t = kh$, h is the sampling time, and the last term is to take the control chattering into account and avoid it in the implementations. The optimized parameters are listed in Table V. One may see that the optimization algorithms may lead to suboptimal solutions. For instance, noncollocated PD regulation for the first and the last angles always lead to a larger cost compared to the collocated PD regulation. However, all these three controllers have the same structure since k_a is always zero for the noncollocated ones. Therefore, k_p and k_d corresponding to the collocated PD should also be selected for the other two controllers which is not the case here. As the result, a larger cost has been obtained for these two noncollocated controllers. This indicates that the designers have to be careful when using the above three optimization algorithms, and that some work to improve the gains calculations remains to be done.

Note that throughout this paper, colors blue, black and red in tables, indicate the best, average and the worst groups. According to Table V, the double-pendulum SMC has achieved the worst results. Apart from the implicit double pendulum SMC and the tracking controllers, that have average results, other methods show good responses at almost the same level. It also should be noted that the SMCs are implemented based on both explicit and implicit discrete-time Euler schemes since the discretization of discontinuous (set-valued) terms may affect the results [17]. Moreover, the single-pendulum controllers are implemented with the first- and the last- sway angles as feedbacks in two different implementations which are indicated by "first" and "last" in the tables. Another observation from Table V is that the implicit discretization of the double-pendulum SMC has achieved a smaller cost than the explicit one.

The simulations have been conducted in Simulink using Simscape Multibody toolbox. The `ode15s` solver has been employed to solve the equations from $t = 0$s to $t = 100$s on the 20-link pendulum system with nominal condition shown in Table III without any disturbance, initial sway, or measurement noise under two different scenarios, i.e., regulation and tracking, in Sections IV-B and IV-C, respectively. Moreover, a worst case scenario has been considered in Section IV-D to evaluate the robustness of the methods.

B. Regulation performances

A trajectory has been selected as follows to evaluate the controllers under the regulation scenario, which is composed of three constant values of acceleration. The reference position for $0 \leq t \leq 4$ is $x_d(t) = 3.5t^2/8 + 1$, for $4 < t < 8$ is $x_d(t) = 3.5t - 6$, for $8 \leq t \leq 12$ is $x_d = -3.5t^2/8 + 10.5t - 34$, for $t > 12$ is $x_d(t) = 29$, and $x_d(t) = 0, \forall t > 12$s. Moreover, the cart starts from the origin, i.e., $x(0) = 0$.

The results of this simulation are summarized in Table VI. Since the system is not disturbed, even the performances of the open-loop methods are comparable with the closed-loop ones. Considering Table VI, one can see that the unshaped control shows the smallest amount of $\tilde{L}_2(e_p)$ after the collocated PD tracking controller. However, this method is not the best in minimizing the cart position error and $\bar{L}_2(e_a)$. According to this simulation, the collocated PD tracking controller looks to be the best in minimizing the payload position under this unperturbed condition. Another observation is that the SMC designed for the double-pendulum system shows the worst responses. It can also be seen from Table VI that the open-loop control methods use the smallest amount of control energy $\tilde{L}_2(F)$ since they do not inject virtual damping to the system.

C. Tracking performance

Another reference trajectory, i.e., $x_d(t) = 5\sin(\omega t)$, has been selected in this section to study the tracking performances of the methods with the same parameters as Section IV-B, and the results are shown in Table VII for $\omega = 0.2$ rad/s. The first observation is that the tracking controllers, i.e., collocated PD tracking and coupling tracking achieve the best results. It can be seen also that for the noncollocated tracking one, i.e., coupling tracking it is better to sense the last sway angle rather than the first one.

According to Table VII it can be seen that the open-loop methods are the worst in the case of tracking for both cart and the payload. On the other hand, as before, the open-loop methods are the best in the case of the control energy and the sway reduction. Similar to the previous case, the SMC designed for the double-pendulum as well as the PD energy with the first angle sensing have achieved the worst results in terms of tracking for both cart and the payload as well as the control energy and sway angles. However, as can be seen, the PD energy can achieve better responses with a sway sensor on the last angle.

The tracking performances of the controllers for the position trajectory $x_d = 5\sin(\omega t)$ with different ω are illustrated in Fig. 2. From this figure, one can see that the open-loop methods are too sensitive to the frequency of the trajectory. Moreover, the tracking controllers show the smallest $\tilde{L}_2(e_p)$ and their responses are nearly insensitive to ω.

D. Worst case regulation scenario

To study the robustness of the controllers, a simulation is conducted under a perturbed condition. The trajectory and the conditions are the same as Section IV-B except for the following perturbations:

- The initial sway angle is $\theta_i = \alpha_i 15^o$ with $\alpha_i = 1$ for $i = 2k$ and $\alpha_i = -1$ for $i = 2k+1$, and $k = 1, 2, \ldots, 9$.
- All measurements are contaminated with 90dB signal-to-noise ratio white noise.
- Damping on the cart is equal to $1000v(t)$N to simulate a kind of friction between the cart and the surface.
- cart and payload disturbances (pulse forces with period 20s and amplitude $\pm$19600N are applied directly to the cart and the payload)

The results of this simulation are shown in Table VIII. While, as before, the open-loop methods, e.g., unshaped input, ZV, and ZVD, show the smallest control effort, they were completely sensitive to the perturbations, and show the worst tracking performances for the cart and payload

TABLE V

OPTIMIZED PARAMETERS

Method	Parameters	Cost (2)
Collocated PD regulation	k_p=8e+02, k_d=3e+04	19161
Quasi-PID	k_p=1e+04, k_d=6e+04, k_i=1e+00, $k_{\phi 1}$=0, $k_{\phi 2}$=4e-04, $\lambda = 5e+04$	18601
Noncollocated PD regulation (first angle)	k_p=1e+04, k_d=4e+04, k_a=0	26400
Noncollocated PD regulation (last angle)	k_p=1e+03, k_d=3e+04, k_a=0	20078
Collocated PD tracking	k_p=2e+02, k_d=2e+04, L_0=3e+03, Z=3e+03, ϕ=0	31548
PD-PD	α_1=1e+04, α_2=4e+04, α_3 =3e+04 , α_4 =-9e-01,	26022
Explicit single-pendulum SMC (first angle)	c_1=4e-02, c_2=0, c_3 =4e-02 , c_4 =0 , k=3e-01 , η =2e-05	25723
Implicit single-pendulum SMC (first angle)	c_1=4e-02, c_2=0, c_3 =4e-02 , c_4 =0 , k=3e-01 , η =2e-05	25720
Explicit single-pendulum SMC (last angle)	c_1=4e-02, c_2=0, c_3 =0 , c_4 =0 , k=3e-01 , η =1e-05	26382
Implicit single-pendulum SMC (last angle)	c_1=4e-02, c_2=0, c_3 =0 , c_4 =0 , k=3e-01 , η =2e-05	26384
Explicit double-pendulum SMC	λ=2e+01, α=3e+00, β=1e+02 , K =6e+03 , c=9e+03	3072729
Implicit double-pendulum SMC	λ=2e+00, α=4e+00, β=3e-08 , K =3e+00 , c=4e-01	46587
PD energy (first angle)	k_p=1e+03, k_d=3e+04, k_q=1e+05 , λ =1e+00 , ζ=4e+00	18806
PD energy (last angle)	k_p=4e+03, k_d=3e+04, k_q=3e+04 , λ =1e-02 , ζ=2e+07	19420
Coupling tracking (first angle)	k_p=5e+03, k_d=7e+03, λ=6e-01	122748
Coupling tracking (last angle)	k_p=6e+03, k_d=1e+04, λ=0	123504

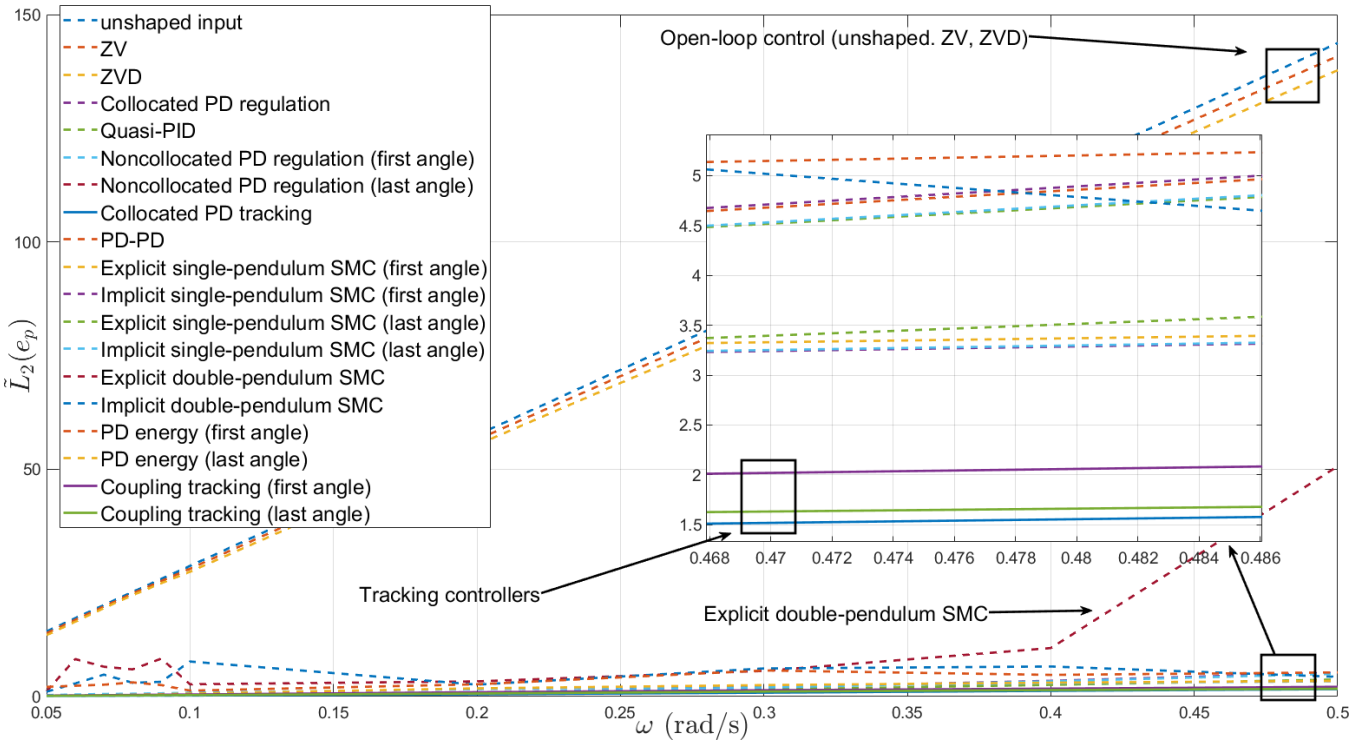

Fig. 2. $\tilde{L}_2$ norms of the payload position tracking error for the trajectory $x_d(t) = 5\sin(\omega t)$

as well as the worst sway control. Another observation from Table VIII is that while the tracking controllers show almost the best responses for both regulation and tracking under the unperturbed cases in Sections IV-B and IV-C, they show the worst responses after the open-loop method and the SMC designed for the double pendulum system. The reason is that, according to Table I, and similar to the open-loop methods, the tracking controllers depend on the feedforward term which decreases their robustness. Moreover, the SMCs designed for the single-pendulum system show the best responses which indicate their robustness. Furthermore, as before, it seems that the controllers designed for the single-pendulum system behave better when the last angle is measured instead of the first one.

V. CONCLUSIONS

Some known controllers are reviewed in case of their structure, feedback, parameters, and stability type. The controllers have been implemented on a model composed of a 20-link pendulum attached to a cart, which can capture both global nonlinearities and the cables' flexibility. The behavior of the controllers for the regulation and the tracking scenarios has been studied under both nominal and perturbed conditions. The implementation of the open-loop schemes is simple and they need the smallest amounts of control energy. However, their other performances like payload positioning are worse than the general behavior of the closed-loop methods especially for the tracking and perturbed conditions. In an unperturbed case, the noncollocated feedback may not

TABLE VI

RESULTS FOR THE REGULATION

Method	$\tilde{L}_2(e_p)$	$\tilde{L}_2(e_c)$	$\tilde{L}_2(e_a)$	$\tilde{L}_2(F)$
Unshaped input	1.08	1.20	7.08	15795
ZV	2.14	2.18	5.59	12611
ZVD	3.13	3.12	4.71	11020
Collocated PD	2.12	2.07	2.22	12924
quasi-PID	1.38	1.27	2.84	15360
Non.CO.PD.Reg. (first)	2.14	2.09	2.21	12857
Non.CO.PD.Reg. (last)	1.37	1.09	3.77	20516
Collocated PD Tracking	0.55	0.35	4.28	18035
PD-PD	1.40	1.11	3.74	20745
SMC-single-first (explicit)	1.39	1.10	3.77	20787
SMC-single-first (implicit)	1.39	1.10	3.77	20787
SMC-single-last (explicit)	1.37	1.09	3.78	20499
SMC-single-last (implicit)	1.37	1.09	3.79	20523
SMC-double (explicit)	21.65	21.64	15.25	99533
SMC-double (implicit)	1.86	1.84	14.10	94108
PD energy (first)	2.00	1.96	2.23	12398
PD energy (last)	2.14	2.10	2.14	12303
Coupling tracking (first)	1.17	1.14	3.96	16161
Coupling tracking (last)	1.11	1.07	4.04	16755

TABLE VII

RESULTS FOR THE TRAJECTORY TRACKING

Method	$\tilde{L}_2(e_p)$	$\tilde{L}_2(e_c)$	$\tilde{L}_2(e_a)$	$\tilde{L}_2(F)$
Unshaped input	57.51	57.51	1.46	8932
ZV	56.48	56.47	1.39	8495
ZVD	55.35	55.34	1.33	8106
Collocated PD	1.64	1.60	1.98	9418
quasi-PID	0.84	0.71	2.54	11523
Non.CO.PD.Reg. (first)	1.66	1.61	1.97	9392
Non.CO.PD.Reg. (last)	0.91	0.73	2.71	12063
Collocated PD Tracking	0.49	0.42	2.00	10024
PD-PD	0.92	0.74	2.59	12064
SMC-single-first (explicit)	0.91	0.73	2.61	12053
SMC-single-first (implicit)	0.91	0.73	2.61	12053
SMC-single-last (explicit)	0.91	0.73	2.72	12062
SMC-single-last (implicit)	0.91	0.73	2.72	12063
SMC-double (explicit)	3.34	3.35	14.05	99541
SMC-double (implicit)	2.62	2.60	21.65	92152
PD energy (first)	2.70	2.48	6.12	24375
PD energy (last)	1.81	1.74	2.07	10165
Coupling tracking (first)	0.96	0.86	1.81	10612
Coupling tracking (last)	0.67	0.59	1.84	10197

TABLE VIII

RESULTS FOR THE WORST-CASE REGULATION SCENARIO

Method	$\tilde{L}_2(e_p)$	$\tilde{L}_2(e_c)$	$\tilde{L}_2(e_a)$	$\tilde{L}_2(F)$
Unshaped input	124.37	124.33	62.51	15797
ZV	126.53	126.51	66.94	12612
ZVD	126.53	126.53	65.63	11020
Collocated PD	3.22	2.98	37.25	24980
quasi-PID	2.14	1.88	35.42	32055
Non.CO.PD.Reg.1	3.25	3.02	37.46	24849
Non.CO.PD.Reg.n	2.40	1.96	36.59	39332
Col.PD.Track	4.14	3.65	40.38	39716
PD-PD	2.52	2.06	36.41	39817
SMC-single-first (explicit)	2.54	2.08	34.75	41155
SMC-single-first (implicit)	2.54	2.08	34.73	41144
SMC-single-last (explicit)	2.40	1.96	36.49	39302
SMC-single-last (implicit)	2.40	1.96	36.66	39358
SMC-double (explicit)	15.38	15.29	31.84	99698
SMC-double (implicit)	6.00	5.85	36.95	95467
PD energy (first)	3.22	2.95	35.85	33915
PD energy (last)	3.37	3.13	37.38	24849
Coupling tracking (first)	9.43	8.54	53.41	66621
Coupling tracking (last)	7.08	6.33	42.89	49187

provide any advantages over the collocated one. However, under the perturbed case, the noncollocated feedback can improve the performances. While the tracking controllers show the best results for the unperturbed case, they behave a kind of less than average in the presence of perturbation since they depend on the feedforward term. Measuring the sway angle for the single-pendulum-based controllers is another issue since according to the results, measuring different angles can change the results. In general, measuring the last angle leads to better results compared to measuring the first one. Moreover, the discretization affects the results corresponding to the double-pendulum SMC, where the implicit method gives better results than the explicit one. Future study will address the 3D operational space case, and the multi-cable case. Testing other cable's models (like FEM ones [18]) and improving the gains tuning optimisation code, are also future goals.

REFERENCES

[1] E. Abdel-Rahman, A. Nayfeh, and Z. Masoud, "Dynamics and control of cranes: A review," *J. Vib. Cont.*, vol. 9, pp. 863–908, 2003.

[2] K.-S. Hong and U. H. Shah, *Dynamics and Control of Industrial Cranes*. Springer, 2019.

[3] L. Ramli, Z. Mohamed, A. M. Abdullahi, H. Jaafar, and I. M. Lazim, "Control strategies for crane systems: A comprehensive review," *Mechanical Systems and Signal Processing*, vol. 95, pp. 1–23, 2017.

[4] H. Chen, B. Xuan, P. Yang, and H. Chen, "A new overhead crane emergency braking method with theoretical analysis and experimental verification," *Nonlinear Dyn.*, vol. 98, no. 3, pp. 2211–2225, 2019.

[5] N. Sun, T. Yang, Y. Fang, Y. Wu, and H. Chen, "Transportation control of double-pendulum cranes with a nonlinear quasi-pid scheme: Design and experiments," *IEEE Trans. on Syst., Man, and Cyb.: Systems*, vol. 49, no. 7, pp. 1408–1418, 2019.

[6] W. He and S. S. Ge, "Cooperative control of a nonuniform gantry crane with constrained tension," *Automatica*, vol. 66, pp. 146–154, 2016.

[7] B. d' Andréa-Novel and J. Coron, "Exponential stabilization of an overhead crane with flexible cable via a backstepping approach," *Automatica*, vol. 36, no. 4, pp. 587–593, 2000.

[8] H. Alli and T. Singh, "Passive control of overhead cranes," in *Proc. 1998 IEEE Int. Conf. on Control Appl.*, vol. 2, 1998, pp. 1046–1050.

[9] M. R. Mojallizadeh, B. Brogliato, and V. Acary, "Time-discretizations of differentiators: Design of implicit algorithms and comparative analysis," *Int. J. Rob. Nonlin. Cont.*, vol. 31, pp. 7679–7723, 2021.

[10] N. Sun and Y. Fang, "New energy analytical results for the regulation of underactuated overhead cranes: An end-effector motion-based approach," *IEEE Trans. Ind. Elec.*, vol. 59, pp. 4723–4734, 2012.

[11] N. Sun and Y. Fang, "Nonlinear tracking control of underactuated cranes with load transferring and lowering: Theory and experimentation," *Automatica*, vol. 50, pp. 2350–2357, 2014.

[12] B. d'Andréa Novel, I. Moyano, and L. Rosier, "Finite-time stabilization of an overhead crane with a flexible cable," *Math. Cont., Sign. Syst.*, vol. 31, no. 2, pp. 1–19, 2019.

[13] D. Qian and J. Yi, "Hierarchical sliding mode control for underactuated cranes," *Springer*, 2016.

[14] L. A. Tuan and S.-G. Lee, "Sliding mode controls of double-pendulum crane systems," *J. Mech. Sci. Tech.*, vol. 27, pp. 1863–1873, 2013.

[15] S. Zhang, X. He, Q. Chen, and Y. Feng, "Improved energy dissipation control of overhead cranes," *Asian J. of Cont.*, vol. 22, no. 4, pp. 1729–1735, 2020.

[16] M. Zhang, X. Ma, X. Rong, R. Song, X. Tian, and Y. Li, "An enhanced coupling nonlinear tracking controller for underactuated 3d overhead crane systems," *Asian J. of Cont.*, vol. 20, no. 5, pp. 1839–1854, 2018.

[17] B. Brogliato and A. Polyakov, "Digital implementation of sliding-mode control via the implicit method: A tutorial," *Int. J. Rob. Nonlin. Cont.*, vol. 31, no. 9, pp. 3528–3586, 2021.

[18] G. Fotland and B. Haugen, "Numerical integration algorithms and constraint formulations for ALE-ANCF cable element," *Mech. Mach. Theo.*, vol. 170, p. 104659, 2022.